MICROSECOND MODEL UPDATING FOR 2D STRUCTURAL SYSTEMS USING THE LOCAL EIGENVALUE MODIFICATION PROCEDURE (LEMP)

Emmanuel A. Ogunniyi [1], Alexander B. Vereen [1], Austin R.J. Downey [1,2]
[1]Department of Mechanical Engineering, University of South Carolina, Columbia, USA
[2]Department of Civil and Environmental Engineering, University of South Carolina, Columbia, USA

UNIVERSITY OF SOUTH CAROLINA

Contents

High-rate Dynamics in the Real-world

Civil Structures Exposed to blast

Samali, B., et al., *Review of the basics of state of the art of blast loading. Asian Journal of Civil Engineering.* (2018).

Automotive safety systems against Collision

airbag deployment

Space shuttle and Aerial Vehicles Prone to In-Flight Anomalies

Hypersonic vehicles

Ballistic packages

Debris approaching space shuttle

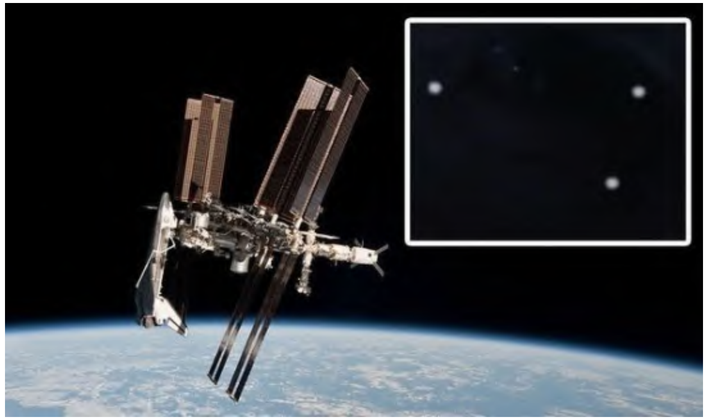

Lightning strikes on aircraft

Fighter jets

Next Generation Electronic Packaging

Thorough collaborations with the AFRL we are working on enabling technology for

- Fuzes with real-time decision-making capabilities
- Fuzes that can “adapt” to their condition
- Fuzes that are resilient to impact (e.g. after an impact, the are just as strong as before)
- Funded through an AFOSR YIP

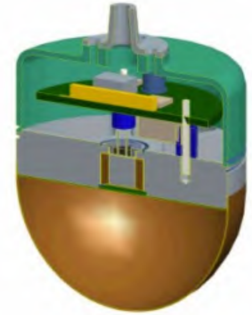

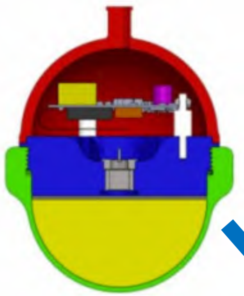

Embedded fuze design are being designed for enhanced safety and reduced cost.

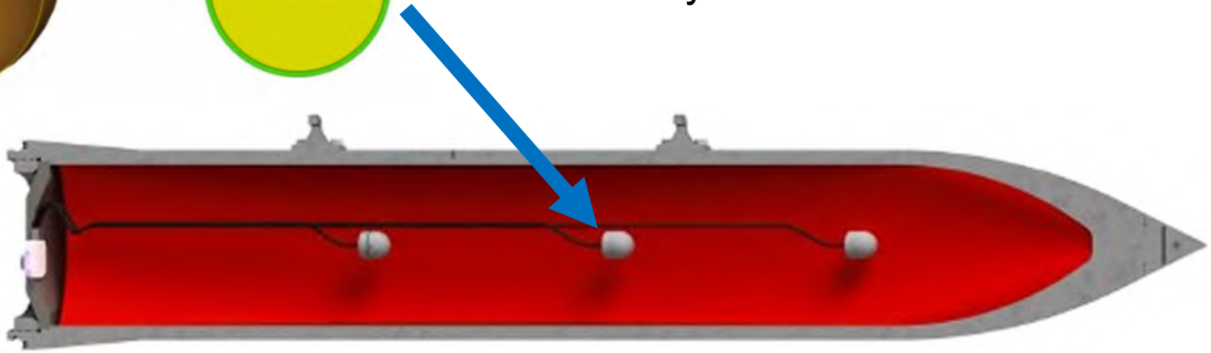

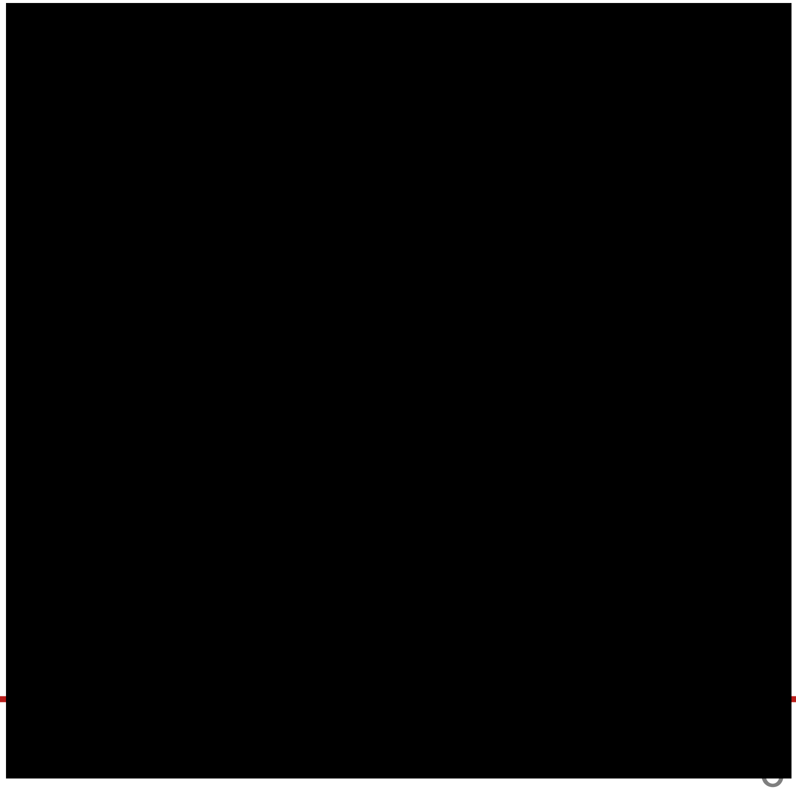

Description of High-rate Dynamics

High-rate (<100ms)

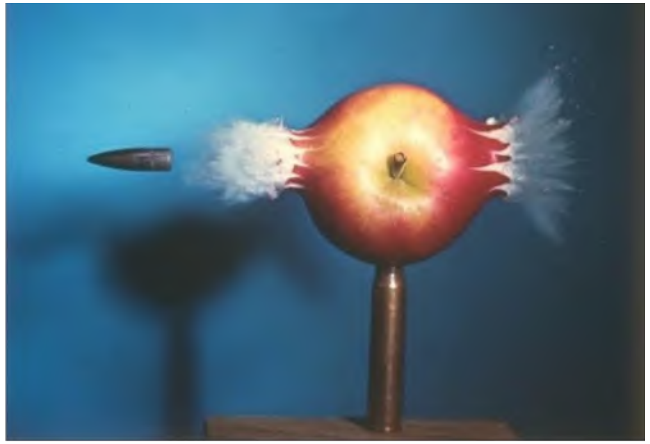

High-amplitude (acceleration > 100 *g*)

The deceleration event in drop tower tests typically lasts for 0.5ms

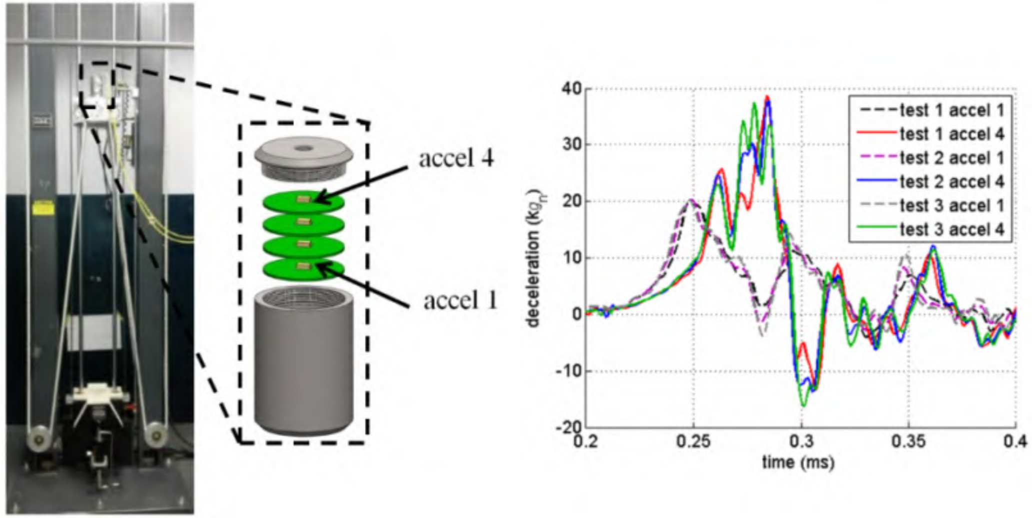

- Large uncertainties in the external loads.
- High levels of nonstationarity and heavy disturbance.
- Generations of unmodeled dynamics from changes in mechanical configuration.

GitHub

Hong, J. et al,. *Introduction to state estimation of high-rate system dynamics*. Sensors, 18(2):217, Jan 2018

Reproducing High-rate Dynamics in Laboratory

DROPBEAR experimental testbed:

- The Dynamic Reproduction of Projectiles in Ballistic Environments for Advanced Research (DROPBEAR) was used to generate the experimental data in this work.
- Cantilever beam with a controllable roller to alter the state.
- Acceleration and pin location are recorded.
- Dataset available on GitHub at: https://github.com/High-Rate-SHM-Working-Group/Dataset-2-DROPBEAR-Acceleration-vs-Roller-Displacement

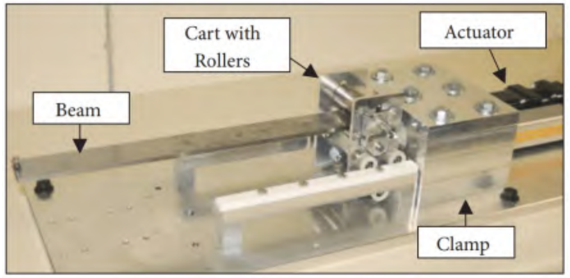

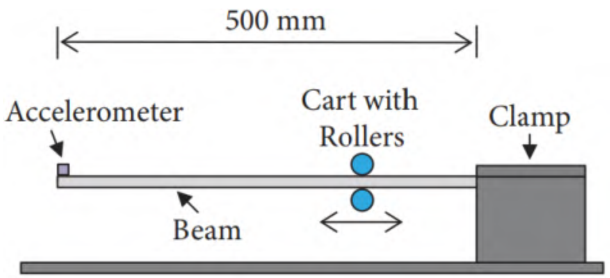

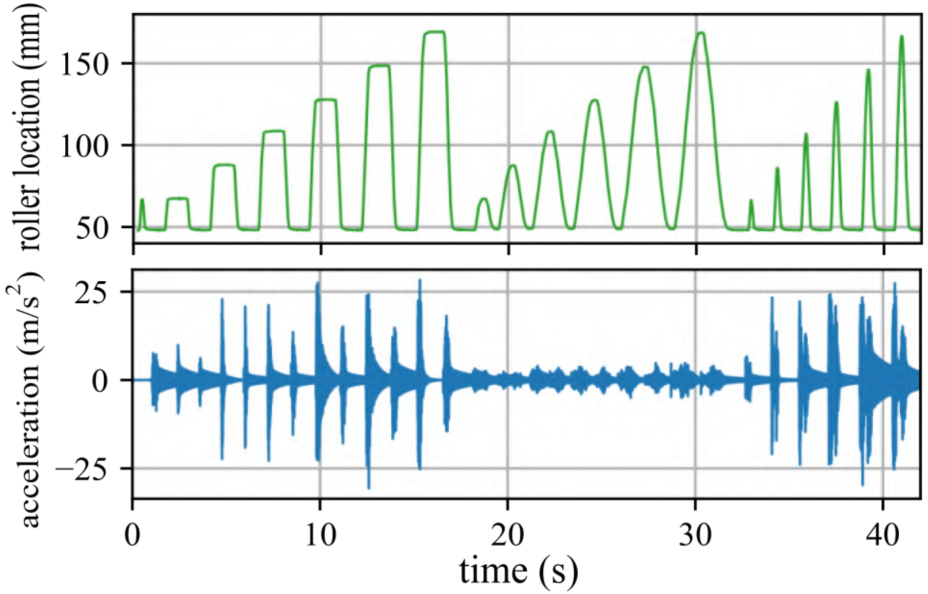

Joyce, B., Dodson, J., Laflamme, S., & Hong, J. *An experimental test bed for developing high-rate structural health monitoring methods*. Shock and Vibration, 2018.

Experimental System used for Validation

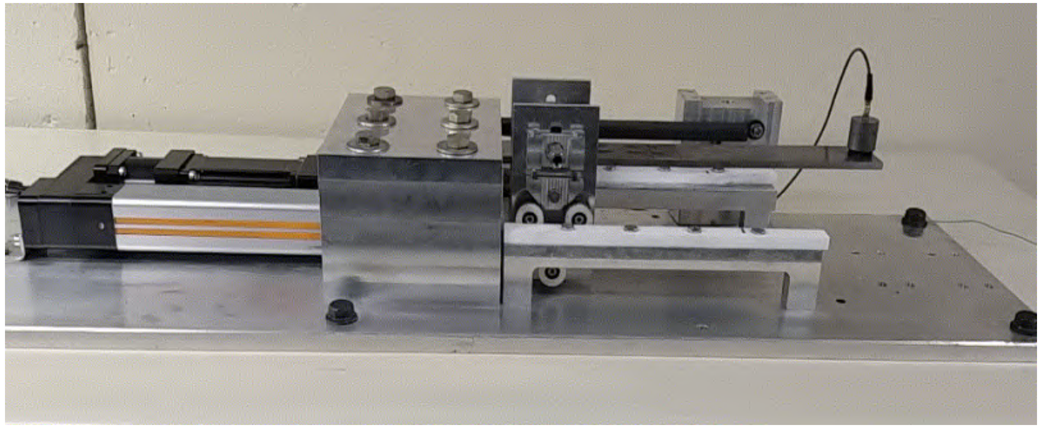

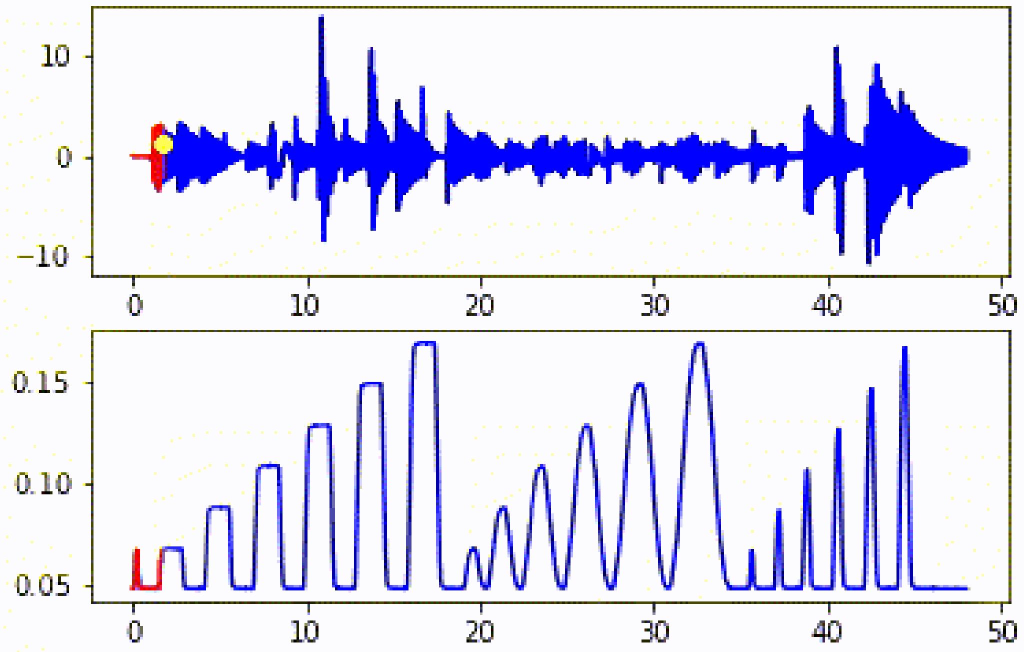

Joyce, B., Dodson, J., Laflamme, S., & Hong, J. *An experimental test bed for developing high-rate structural health monitoring methods*. Shock and Vibration, 2018.

Real-time FEA model updating (1D)

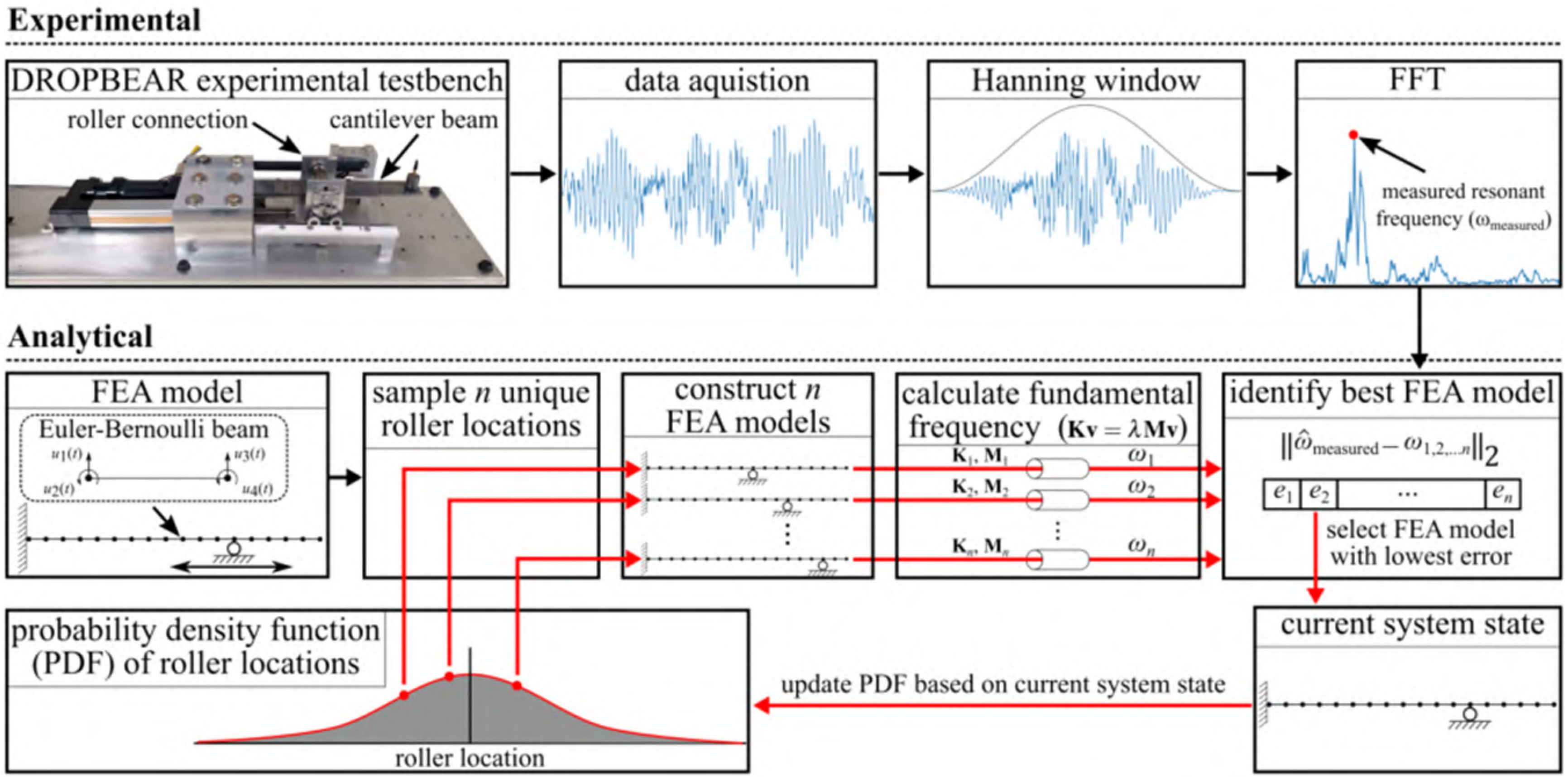

Downey A., et al,. "Millisecond Model Updating for Structures Experiencing Unmodeled High-Rate Dynamic Events" *Mechanical Systems and Signal Processing* ***138***, 2020

Real-time FEA model updating Results

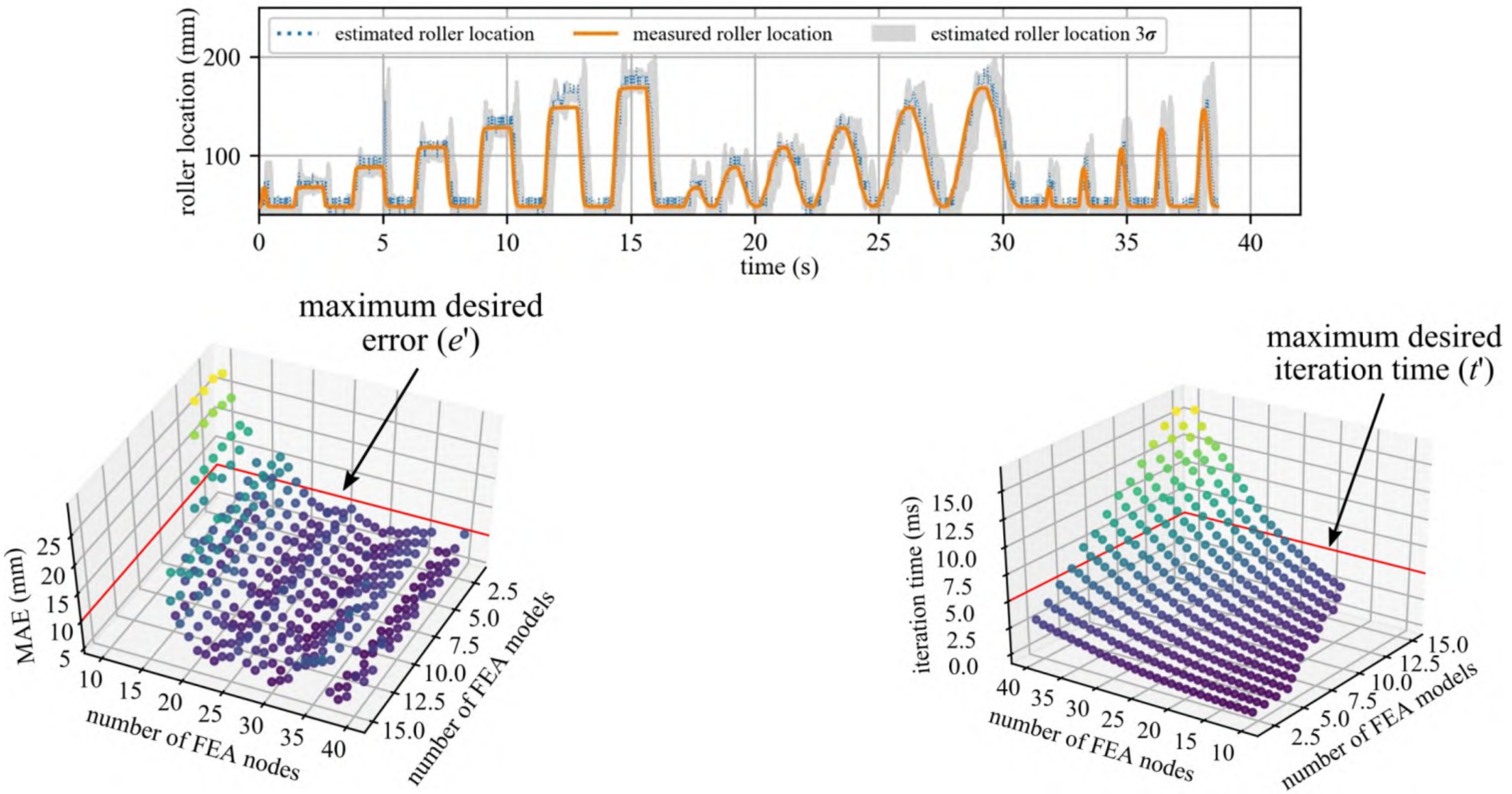

Downey A., et al,. "Millisecond Model Updating for Structures Experiencing Unmodeled High-Rate Dynamic Events" *Mechanical Systems and Signal Processing* ***138***, 2020

FEA Computation speed for the DROPBEAR

General Eigenvalue solutions accurately estimates the state of the DROPBEAR

Solving for system's frequencies accounted for 90% of algorithm iteration time

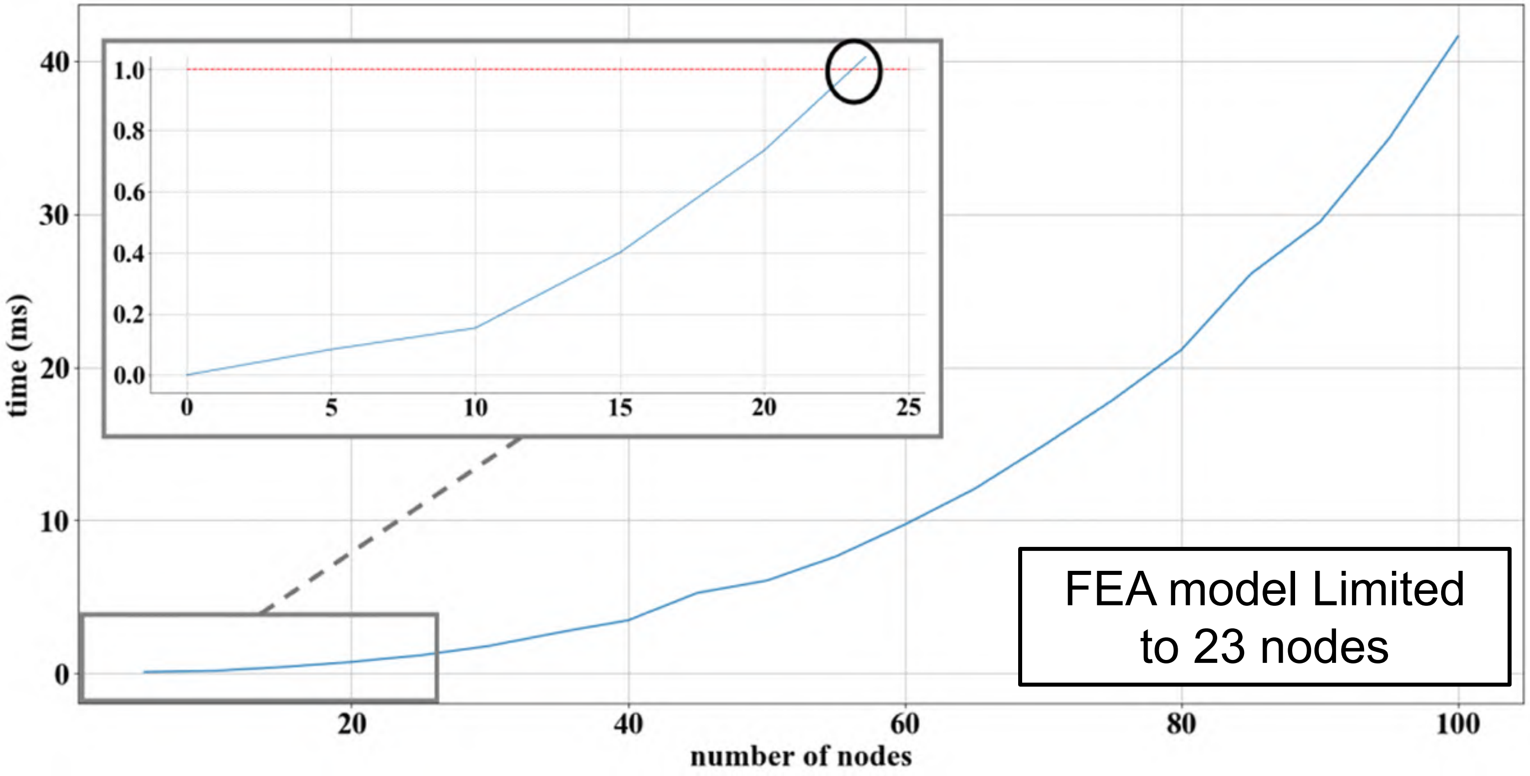

FEA model Limited to 23 nodes

Carroll, M., Downey, A., Dodson, J., Hong, J. and Scheppegrell, J., "Analysis of Computation Speeds of Eigenvalue Solutions for High-Rate Structural Health Monitoring."

Local Eigenvalue Modification Procedure (LEMP)

- Developed by Wesseinburger in 1968
- Identifies physical changes to the system such as mass, stiffness or damping using changes such as frequencies or mode shapes
- Model the altered state as a mixture of the initial state and changes made to the initial state
- Reduces the GE equation to a set of second-order equations

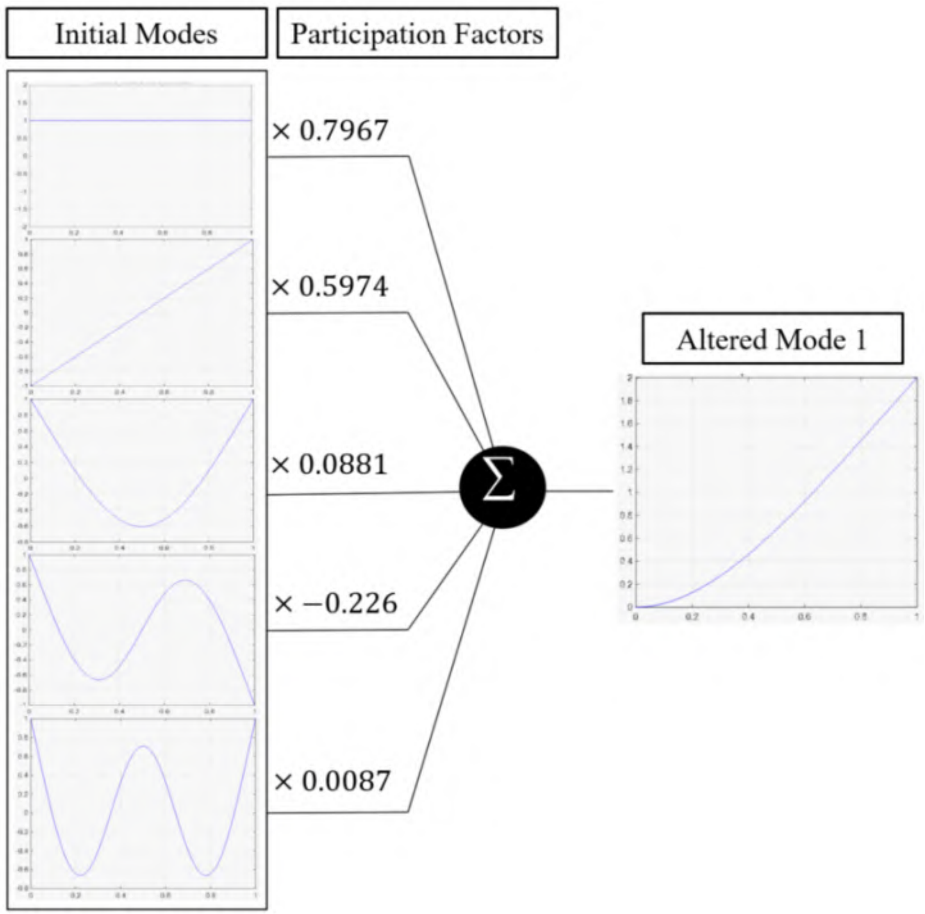

Avitabile, P., "*Twenty Years of Structural Dynamic Modification- A Review*," *Sound and Vibration,* pp. 14-25. 2003
Drnek, C. R., "*Local eigenvalue modification procedure for real-time model updating of structures experiencing high-rate dynamic events*," (2020).

Local Eigenvalue Modification Procedure (LEMP)

n independent single DOF systems representing the initial state

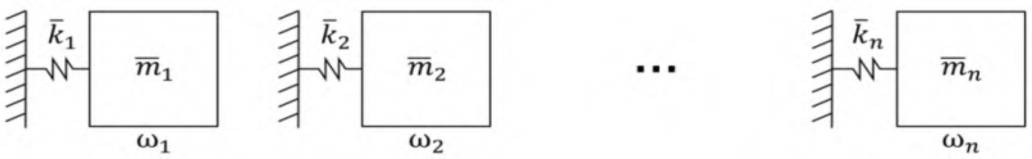

Coupled single DOF systems representing the altered state

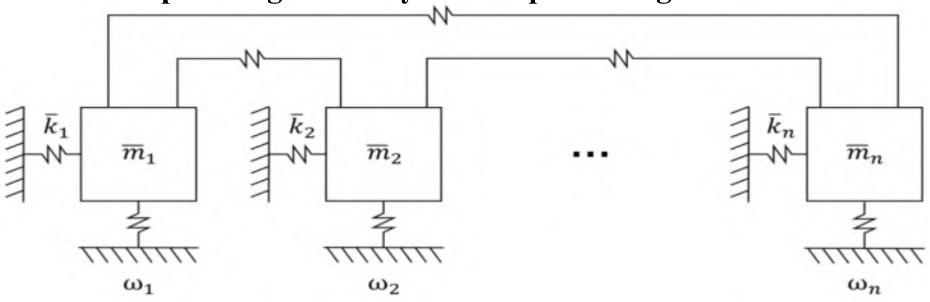

	Initial State	Modification	Altered State	
Physical Space	$[\mathbf{M}_1], [\mathbf{K}_1]$	$[\Delta\mathbf{M}_{12}], [\Delta\mathbf{K}_{12}]$	$[\mathbf{M}_2], [\mathbf{K}_2]$	*'n'* Physical DOF
Modal Transformation	$\{x\} = [U_1]\{p_1\}$	$$\frac{-1}{\alpha} = \sum_{r=1}^{m} \frac{v_r^2}{\omega_r^2 - \Omega_r^2}$$ **Solved using Divide and Conquer method**	$\{x\} = [U_2]\{p_2\}$	*m<<n*
Modal Space	$[\omega_1^2], [U_1]$	$\{p_1\} = [U_{12}]\{p_2\}$	$[\Omega_2^2], [U_2]$	*'m'* Modal DOF

Avitabile, P., "*Twenty Years of Structural Dynamic Modification- A Review*," *Sound and Vibration*, pp. 14-25. 2003
Drnek, C. R., "*Local eigenvalue modification procedure for real-time model updating of structures experiencing high-rate dynamic events*," (2020).

Current methodology

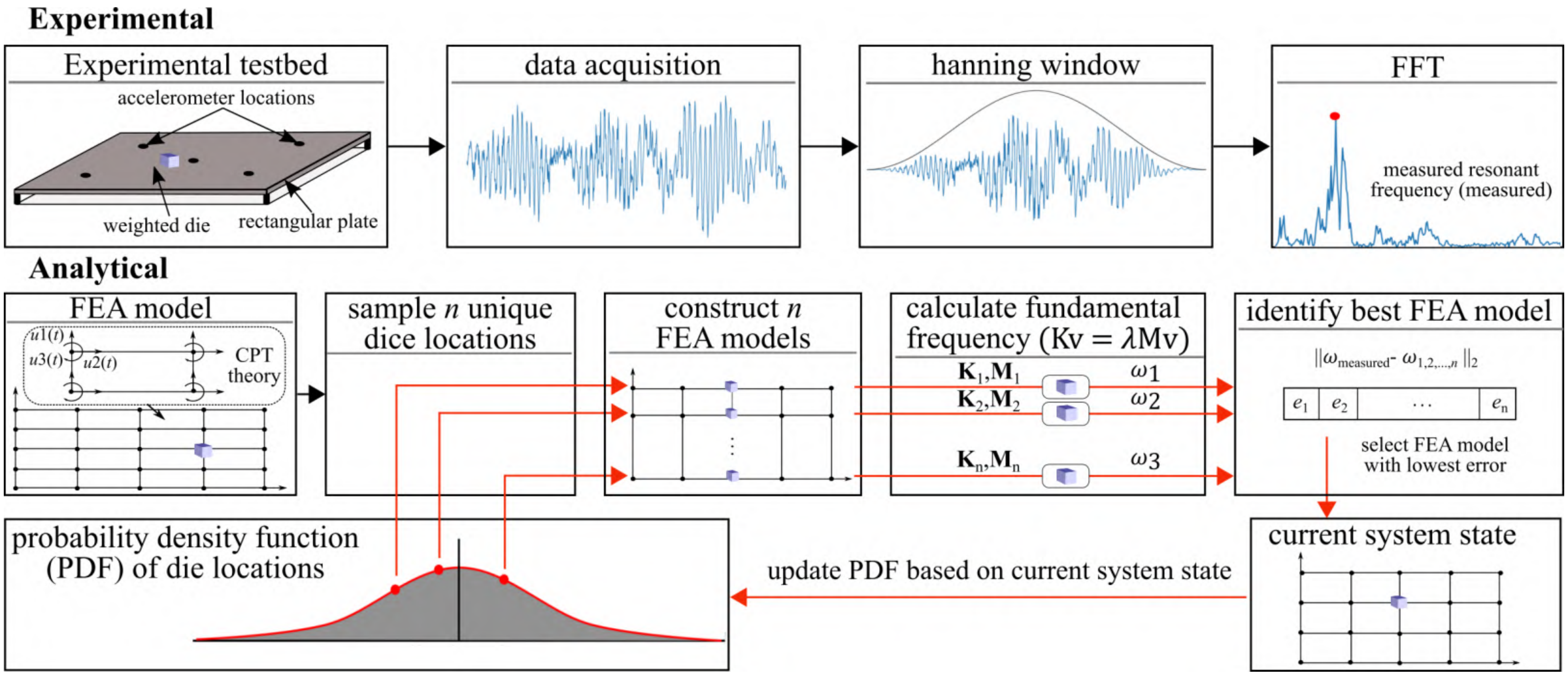

1D vs 2D Structural systems

1D

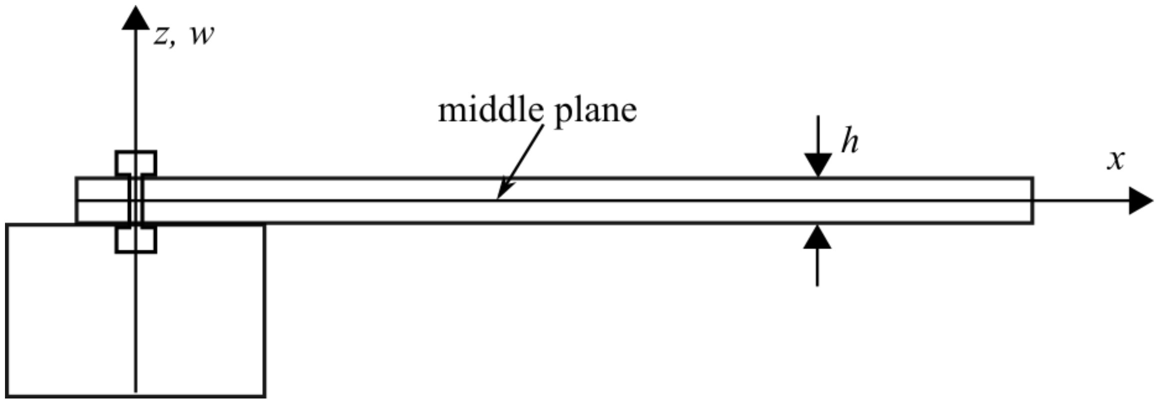

2D

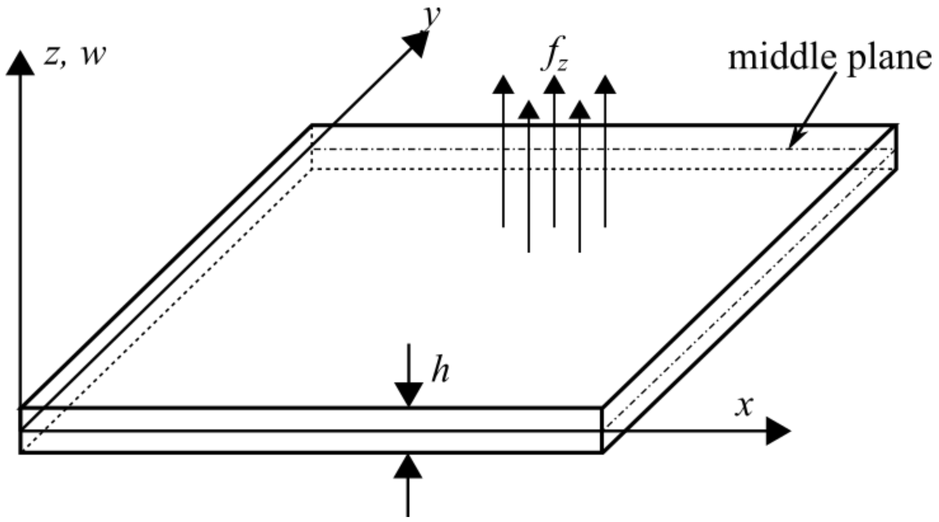

1D vs 2D Node construction

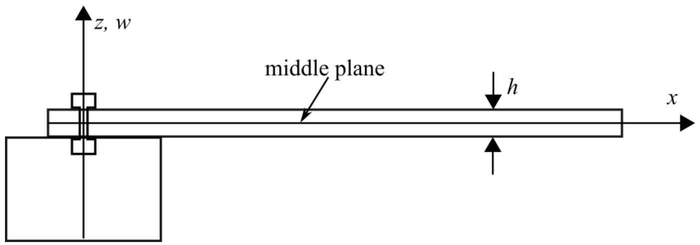

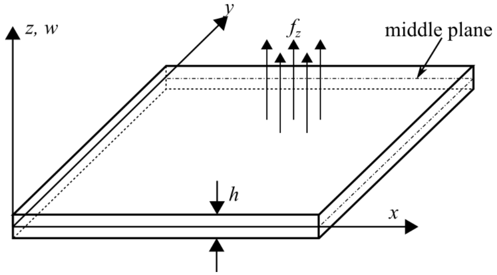

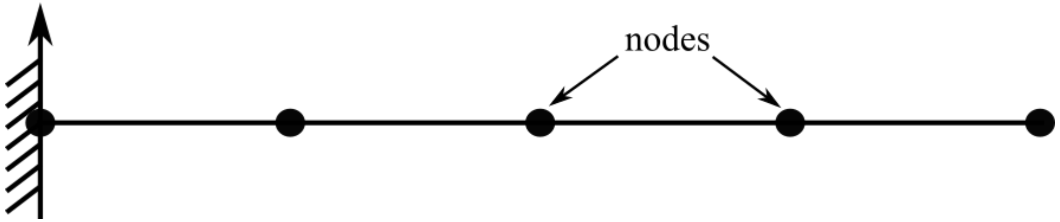

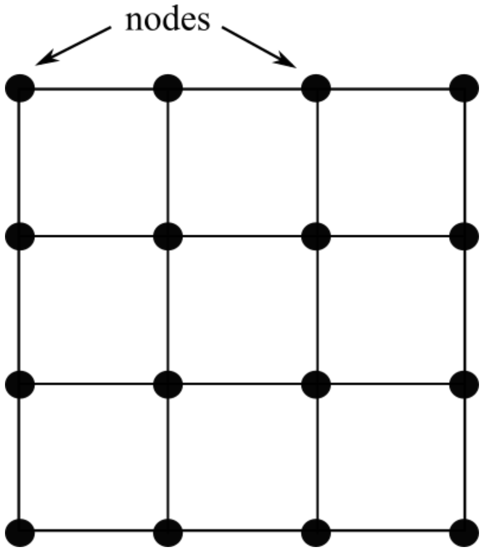

2D Model Formulation

Shell element

Three translational displacements in the *x*, *y*, and *z* directions, and three rotational deformations with respect to the *x*, *y*, and *z* axes.

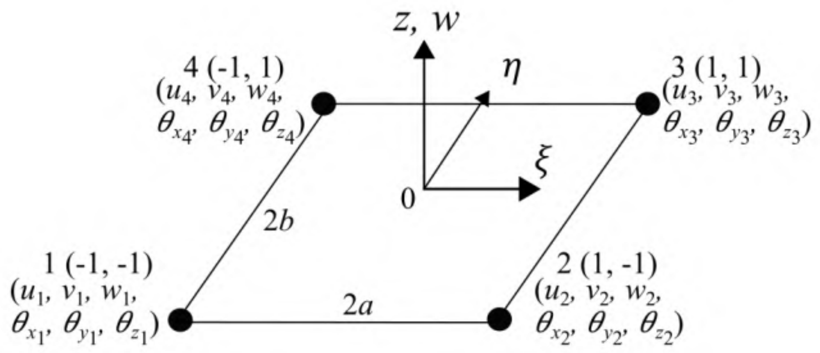

$$\mathbf{d}_e = \begin{Bmatrix} \mathbf{d}_1 \\ \mathbf{d}_2 \\ \mathbf{d}_3 \\ \mathbf{d}_4 \end{Bmatrix} \begin{matrix} \text{node 1} \\ \text{node 2} \\ \text{node 3} \\ \text{node 4} \end{matrix}$$

where $\mathbf{d}_i$ (i=1, 2, 3, 4) are the displacement vector at node i:

$$\mathbf{d}_i = \begin{Bmatrix} u_i \\ v_i \\ w_i \\ \theta_{xi} \\ \theta_{yi} \\ \theta_{zi} \end{Bmatrix} \begin{matrix} \text{displacement in } x \text{ direction} \\ \text{displacement in } y \text{ direction} \\ \text{displacement in } z \text{ direction} \\ \text{rotation about } x\text{-axis} \\ \text{rotation about } y\text{-axis} \\ \text{rotation about } z\text{-axis} \end{matrix}$$

2D Model Formulation

2D solid element is used for the membrane effects, corresponding to DOFs of *u* and *v*.

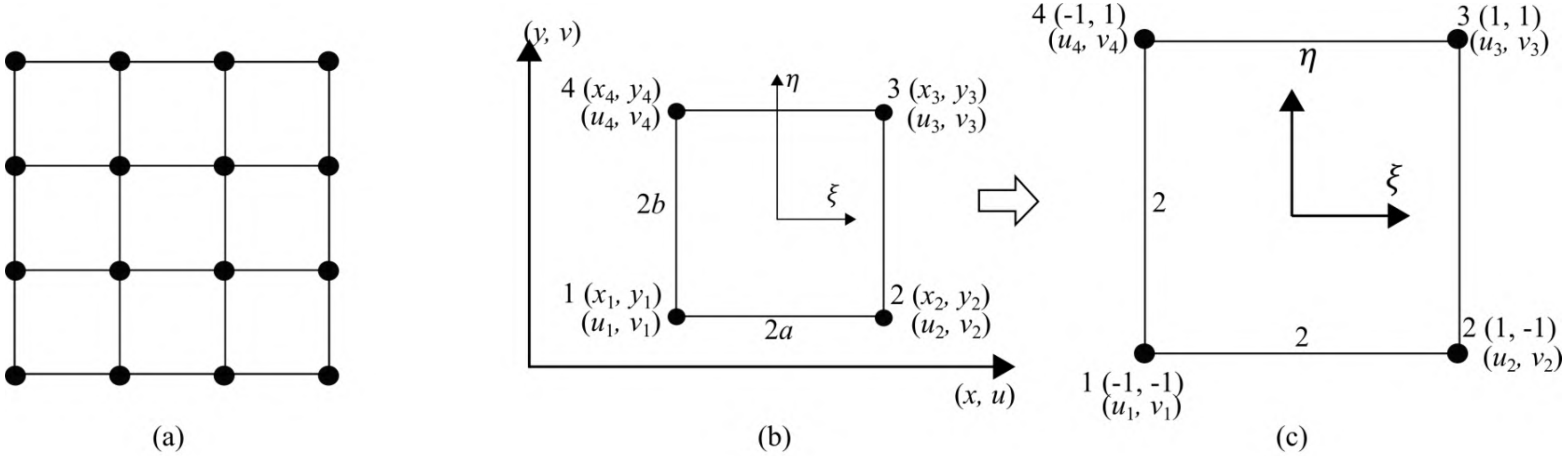

Shell element formation and its coordinate system where; (a) represents the nodal construction on the element; (b) shows the coordinate system of a 2D solid element with 2 DOFs; (c) shows the transformation of the coordinate system with dimension

2D Model Formulation

Rectangular plate element is used for the bending effects, corresponding to DOFs of w and θx, θy.

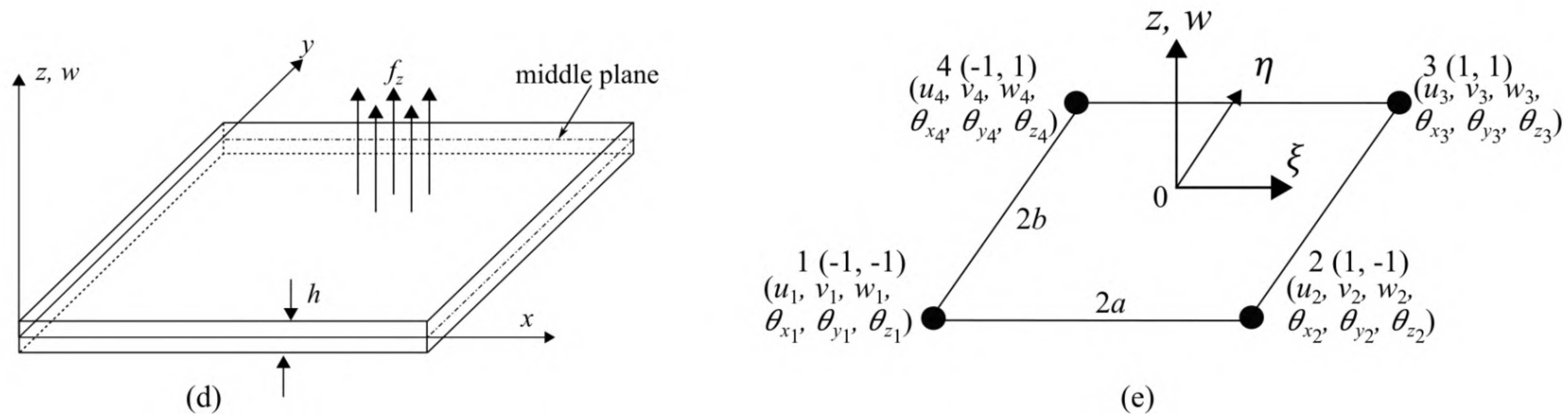

Shell element formation and its coordinate system where; (d) depicts a plate structure, and; (e) is the shell coordinate system that combines the 2D solid element and plate with six DOFs

2D Model Formulation

Modeling steps

1. Construction of shape functions matrix **N**

2. Formulation of the strain matrix for 2D element B, and 2D plate, B_I and B_O.

3. Calculation of k_e and m_e using shape functions N and strain matrix in step 2.

2D Model Formulation

STEP 1. Construction of shape functions matrix N that satisfies Eqs. 1 and 2

2D element

$$\mathbf{N}_e = \begin{bmatrix} N_1 & 0 & N_2 & 0 & N_3 & 0 & N_4 & 0 \\ 0 & N_1 & 0 & N_2 & 0 & N_3 & 0 & N_4 \end{bmatrix} \quad (1)$$

2D plate

$$\mathbf{N}_p = \begin{bmatrix} N_1 & 0 & 0 & N_2 & 0 & 0 & N_3 & 0 & 0 & N_4 & 0 & 0 \\ 0 & N_1 & 0 & 0 & N_2 & 0 & 0 & N_3 & 0 & 0 & N_4 & 0 \\ 0 & 0 & N_1 & 0 & 0 & N_2 & 0 & 0 & N_3 & 0 & 0 & N_4 \end{bmatrix} \quad (2)$$

Subscript

e – 2D element
p – 2D plate

2D Model Formulation

STEP 2. Formulation of the strain matrix for 2D element B, Eq. 3 and 2D plate, B_I and B_O shown in Eqs. 4 and 5.

2D element

$$\mathbf{B} = \mathbf{LN} = \frac{1}{4}\begin{bmatrix} -\frac{1-\eta}{a} & 0 & \frac{1-\eta}{a} & 0 & \frac{1+\eta}{a} & 0 & -\frac{1+\eta}{a} & 0 \\ 0 & -\frac{1-\xi}{b} & 0 & -\frac{1+\xi}{b} & 0 & \frac{1+\xi}{b} & 0 & \frac{1-\xi}{b} \\ -\frac{1-\xi}{b} & -\frac{1-\eta}{a} & -\frac{1+\xi}{b} & \frac{1-\eta}{a} & \frac{1+\xi}{b} & \frac{1+\eta}{a} & \frac{1-\xi}{b} & -\frac{1+\eta}{a} \end{bmatrix} \tag{3}$$

2D plate

$$\mathbf{B}^{\mathrm{I}} = \begin{bmatrix}\mathbf{B}_1^{\mathrm{I}} & \mathbf{B}_2^{\mathrm{I}} & \mathbf{B}_3^{\mathrm{I}} & \mathbf{B}_4^{\mathrm{I}}\end{bmatrix}, \qquad \mathbf{B}_{\mathrm{j}}^{\mathrm{I}} = \begin{bmatrix} 0 & 0 & -\partial N_j/\partial x \\ 0 & \partial N_j/\partial x & 0 \\ 0 & \partial N_j/\partial y & -\partial N_j \partial y \end{bmatrix} \tag{4}$$

$$\mathbf{B}^{\mathrm{O}} = \begin{bmatrix}\mathbf{B}_1^{\mathrm{O}} & \mathbf{B}_2^{\mathrm{O}} & \mathbf{B}_3^{0} & \mathbf{B}_4^{0}\end{bmatrix}, \qquad \mathbf{B}_{\mathrm{j}}^{\mathrm{O}} = \begin{bmatrix} \partial N_j/\partial x & 0 & N_j \\ \partial N_j/\partial y & -N_j & 0 \end{bmatrix} \tag{5}$$

2D Model Formulation

STEP 3. Calculation of k_e and m_e using shape functions N and strain matrix in step 2. to obtain Eqs. 6 and 7.

mass matrix

$$\mathbf{m}_\mathrm{e} = \int_A h\rho \mathbf{N}^\mathrm{T}\mathbf{N}\mathrm{dA}, \qquad \mathbf{m}_\mathrm{p} = \int_{A_p} \mathbf{N}^\mathrm{T}\mathbf{I}\mathbf{N}\mathrm{dA} \qquad (6)$$

$$\mathbf{I} = \begin{bmatrix} \rho h & 0 & 0 \\ 0 & \rho h^3/12 & 0 \\ 0 & 0 & \rho h^3/12 \end{bmatrix}$$

stiffness matrix

$$\mathbf{k}_\mathrm{e} = \int_A h\mathbf{B}^\mathrm{T}\mathbf{c}\mathbf{B}\mathrm{dA}, \qquad \mathbf{k}_\mathrm{p} = \int_{A_p} \frac{h^3}{12}\left[\mathbf{B}^\mathrm{I}\right]^\mathrm{T}\mathbf{c}\mathbf{B}^\mathrm{I}dA + \int_{A_p} \kappa h \left[\mathbf{B}^\mathrm{O}\right]^\mathrm{T}\mathbf{c}_s\mathbf{B}^\mathrm{O}dA \qquad (7)$$

2D Model Formulation

Mass matrix superposition

The mass matrix for the 2D solid element is used for the membrane effects, corresponding to DOFs of *u* and *v*.

$$
\mathbf{m}_e^m = \begin{array}{c} \begin{array}{cccc} \text{node1} & \text{node2} & \text{node3} & \text{node4} \end{array} \\ \begin{bmatrix} \mathbf{m}_{11}^m & \mathbf{m}_{12}^m & \mathbf{m}_{13}^m & \mathbf{m}_{14}^m \\ \mathbf{m}_{21}^m & \mathbf{m}_{22}^m & \mathbf{m}_{23}^m & \mathbf{m}_{24}^m \\ \mathbf{m}_{31}^m & \mathbf{m}_{32}^m & \mathbf{m}_{33}^m & \mathbf{m}_{34}^m \\ \mathbf{m}_{41}^m & \mathbf{m}_{42}^m & \mathbf{m}_{43}^m & \mathbf{m}_{44}^m \end{bmatrix} \end{array} \begin{array}{l} \\ \text{node1} \\ \text{node2} \\ \text{node3} \\ \text{node4} \end{array}
$$

Where m_{ij} is a 2x2 matrix

$$
\mathbf{m} = \left[\begin{array}{ccc|ccc|ccc|ccc}
\multicolumn{3}{c}{\text{node 1}} & \multicolumn{3}{c}{\text{node 2}} & \multicolumn{3}{c}{\text{node 3}} & \multicolumn{3}{c}{\text{node 4}} \\
\mathbf{m}_{11}^m & \mathbf{0} & 0 & \mathbf{m}_{12}^m & \mathbf{0} & 0 & \mathbf{m}_{13}^m & \mathbf{0} & 0 & \mathbf{m}_{14}^m & \mathbf{0} & 0 \\
\mathbf{0} & \mathbf{m}_{11}^b & 0 & \mathbf{0} & \mathbf{m}_{12}^b & 0 & \mathbf{0} & \mathbf{m}_{13}^b & 0 & \mathbf{0} & \mathbf{m}_{14}^b & 0 \\
0 & 0 & 0 & 0 & 0 & 0 & 0 & 0 & 0 & 0 & 0 & 0 \\
\mathbf{m}_{21}^m & \mathbf{0} & 0 & \mathbf{m}_{22}^m & \mathbf{0} & 0 & \mathbf{m}_{23}^m & \mathbf{0} & 0 & \mathbf{m}_{24}^m & \mathbf{0} & 0 \\
\mathbf{0} & \mathbf{m}_{21}^b & 0 & \mathbf{0} & \mathbf{m}_{23}^b & 0 & \mathbf{0} & \mathbf{m}_{23}^b & 0 & \mathbf{0} & \mathbf{m}_{24}^b & 0 \\
0 & 0 & 0 & 0 & 0 & 0 & 0 & 0 & 0 & 0 & 0 & 0 \\
\mathbf{m}_{31}^m & \mathbf{0} & 0 & \mathbf{m}_{32}^m & \mathbf{0} & 0 & \mathbf{m}_{33}^m & \mathbf{0} & 0 & \mathbf{m}_{34}^m & \mathbf{0} & 0 \\
\mathbf{0} & \mathbf{m}_{31}^b & 0 & \mathbf{0} & \mathbf{m}_{33}^b & 0 & \mathbf{0} & \mathbf{m}_{33}^b & 0 & \mathbf{0} & \mathbf{m}_{34}^b & 0 \\
0 & 0 & 0 & 0 & 0 & 0 & 0 & 0 & 0 & 0 & 0 & 0 \\
\mathbf{m}_{41}^m & \mathbf{0} & 0 & \mathbf{m}_{44}^m & \mathbf{0} & 0 & \mathbf{m}_{43}^m & \mathbf{0} & 0 & \mathbf{m}_{44}^m & \mathbf{0} & 0 \\
\mathbf{0} & \mathbf{m}_{41}^b & 0 & \mathbf{0} & \mathbf{m}_{43}^b & 0 & \mathbf{0} & \mathbf{m}_{43}^b & 0 & \mathbf{0} & \mathbf{m}_{44}^b & 0 \\
0 & 0 & 0 & 0 & 0 & 0 & 0 & 0 & 0 & 0 & 0 & 0
\end{array} \right]
\begin{array}{l} \\ \left.\begin{array}{l} \\ \\ \\ \end{array}\right\} \text{node 1} \\ \left.\begin{array}{l} \\ \\ \\ \end{array}\right\} \text{node 2} \\ \left.\begin{array}{l} \\ \\ \\ \end{array}\right\} \text{node 3} \\ \left.\begin{array}{l} \\ \\ \\ \end{array}\right\} \text{node 4} \end{array}
$$

The mass matrix for a rectangular plate element is used for the bending effects, corresponding to DOFs of *w* and θx, θy.

$$
\mathbf{m}_p^b = \begin{array}{c} \begin{array}{cccc} \text{node1} & \text{node2} & \text{node3} & \text{node4} \end{array} \\ \begin{bmatrix} \mathbf{m}_{11}^b & \mathbf{m}_{12}^b & \mathbf{m}_{13}^b & \mathbf{m}_{14}^b \\ \mathbf{m}_{21}^b & \mathbf{m}_{22}^b & \mathbf{m}_{23}^b & \mathbf{m}_{24}^b \\ \mathbf{m}_{31}^b & \mathbf{m}_{32}^b & \mathbf{m}_{33}^b & \mathbf{m}_{34}^b \\ \mathbf{m}_{41}^b & \mathbf{m}_{42}^b & \mathbf{m}_{43}^b & \mathbf{m}_{44}^b \end{bmatrix} \end{array} \begin{array}{l} \\ \text{node1} \\ \text{node2} \\ \text{node3} \\ \text{node4} \end{array}
$$

Where m_{ij} is a 3x3 matrix

2D Model Formulation

Stiffness matrix superposition

The stiffness matrix for a 2D solid, rectangular element is used to account for the membrane effects of the element, which corresponds to DOFs of u and v.

$$\mathbf{k}_e^m = \begin{array}{c} \begin{array}{cccc} \text{node 1} & \text{node 2} & \text{node 3} & \text{node 4} \end{array} \\ \begin{bmatrix} \mathbf{k}_{11}^m & \mathbf{k}_{12}^m & \mathbf{k}_{13}^m & \mathbf{k}_{14}^m \\ \mathbf{k}_{21}^m & \mathbf{k}_{22}^m & \mathbf{k}_{23}^m & \mathbf{k}_{24}^m \\ \mathbf{k}_{31}^m & \mathbf{k}_{32}^m & \mathbf{k}_{33}^m & \mathbf{k}_{34}^m \\ \mathbf{k}_{41}^m & \mathbf{k}_{42}^m & \mathbf{k}_{43}^m & \mathbf{k}_{44}^m \end{bmatrix} \end{array} \begin{array}{l} \text{node 1} \\ \text{node 2} \\ \text{node 3} \\ \text{node 4} \end{array}$$

$$\mathbf{k} = \begin{array}{c} \begin{array}{cccc} \text{node 1} & \text{node 2} & \text{node 3} & \text{node 4} \end{array} \\ \begin{bmatrix} \mathbf{k}_{11}^m & \mathbf{0} & 0 & \mathbf{k}_{12}^m & \mathbf{0} & 0 & \mathbf{k}_{13}^m & \mathbf{0} & 0 & \mathbf{k}_{14}^m & \mathbf{0} & 0 \\ \mathbf{0} & \mathbf{k}_{11}^b & 0 & \mathbf{0} & \mathbf{k}_{12}^b & 0 & \mathbf{0} & \mathbf{k}_{13}^b & 0 & \mathbf{0} & \mathbf{k}_{14}^b & 0 \\ 0 & 0 & 0 & 0 & 0 & 0 & 0 & 0 & 0 & 0 & 0 & 0 \\ \mathbf{k}_{21}^m & \mathbf{0} & 0 & \mathbf{k}_{22}^m & \mathbf{0} & 0 & \mathbf{k}_{23}^m & \mathbf{0} & 0 & \mathbf{k}_{24}^m & \mathbf{0} & 0 \\ \mathbf{0} & \mathbf{k}_{21}^b & 0 & \mathbf{0} & \mathbf{k}_{23}^b & 0 & \mathbf{0} & \mathbf{k}_{23}^b & 0 & \mathbf{0} & \mathbf{k}_{24}^b & 0 \\ 0 & 0 & 0 & 0 & 0 & 0 & 0 & 0 & 0 & 0 & 0 & 0 \\ \mathbf{k}_{31}^m & \mathbf{0} & 0 & \mathbf{k}_{32}^m & \mathbf{0} & 0 & \mathbf{k}_{33}^m & \mathbf{0} & 0 & \mathbf{k}_{34}^m & \mathbf{0} & 0 \\ \mathbf{0} & \mathbf{k}_{31}^b & 0 & \mathbf{0} & \mathbf{k}_{33}^b & 0 & \mathbf{0} & \mathbf{k}_{33}^b & 0 & \mathbf{0} & \mathbf{k}_{34}^b & 0 \\ 0 & 0 & 0 & 0 & 0 & 0 & 0 & 0 & 0 & 0 & 0 & 0 \\ \mathbf{k}_{41}^m & \mathbf{0} & 0 & \mathbf{k}_{44}^m & \mathbf{0} & 0 & \mathbf{k}_{43}^m & \mathbf{0} & 0 & \mathbf{k}_{44}^m & \mathbf{0} & 0 \\ \mathbf{0} & \mathbf{k}_{41}^b & 0 & \mathbf{0} & \mathbf{k}_{43}^b & 0 & \mathbf{0} & \mathbf{k}_{43}^b & 0 & \mathbf{0} & \mathbf{k}_{44}^b & 0 \\ 0 & 0 & 0 & 0 & 0 & 0 & 0 & 0 & 0 & 0 & 0 & 0 \end{bmatrix} \end{array} \begin{array}{l} \text{node 1} \\ \text{node 2} \\ \text{node 3} \\ \text{node 4} \end{array}$$

The stiffness matrix for a rectangular plate element is used for the bending effects, corresponding to DOFs of w and θx, θy.

$$\mathbf{k}_p^b = \begin{array}{c} \begin{array}{cccc} \text{node 1} & \text{node 2} & \text{node 3} & \text{node 4} \end{array} \\ \begin{bmatrix} \mathbf{k}_{11}^b & \mathbf{k}_{12}^b & \mathbf{k}_{13}^b & \mathbf{k}_{14}^b \\ \mathbf{k}_{21}^b & \mathbf{k}_{22}^b & \mathbf{k}_{23}^b & \mathbf{k}_{24}^b \\ \mathbf{k}_{31}^b & \mathbf{k}_{32}^b & \mathbf{k}_{33}^b & \mathbf{k}_{34}^b \\ \mathbf{k}_{41}^b & \mathbf{k}_{42}^b & \mathbf{k}_{43}^b & \mathbf{k}_{44}^b \end{bmatrix} \end{array} \begin{array}{l} \text{node 1} \\ \text{node 2} \\ \text{node 3} \\ \text{node 4} \end{array}$$

2D Model Formulation

Elements in the global coordinate system

$$\mathbf{K}_e = \mathbf{T}^T \mathbf{k}_e \mathbf{T}$$

$$\mathbf{M}_e = \mathbf{T}^T \mathbf{m}_e \mathbf{T}$$

$$\mathbf{T} = \begin{bmatrix} \mathbf{T}_3 & \mathbf{0} & \mathbf{0} & \mathbf{0} & \mathbf{0} & \mathbf{0} & \mathbf{0} & \mathbf{0} \\ \mathbf{0} & \mathbf{T}_3 & \mathbf{0} & \mathbf{0} & \mathbf{0} & \mathbf{0} & \mathbf{0} & \mathbf{0} \\ \mathbf{0} & \mathbf{0} & \mathbf{T}_3 & \mathbf{0} & \mathbf{0} & \mathbf{0} & \mathbf{0} & \mathbf{0} \\ \mathbf{0} & \mathbf{0} & \mathbf{0} & \mathbf{T}_3 & \mathbf{0} & \mathbf{0} & \mathbf{0} & \mathbf{0} \\ \mathbf{0} & \mathbf{0} & \mathbf{0} & \mathbf{0} & \mathbf{T}_3 & \mathbf{0} & \mathbf{0} & \mathbf{0} \\ \mathbf{0} & \mathbf{0} & \mathbf{0} & \mathbf{0} & \mathbf{0} & \mathbf{T}_3 & \mathbf{0} & \mathbf{0} \\ \mathbf{0} & \mathbf{0} & \mathbf{0} & \mathbf{0} & \mathbf{0} & \mathbf{0} & \mathbf{T}_3 & \mathbf{0} \\ \mathbf{0} & \mathbf{0} & \mathbf{0} & \mathbf{0} & \mathbf{0} & \mathbf{0} & \mathbf{0} & \mathbf{T}_3 \end{bmatrix}_{24\times 24}$$

$\mathbf{T}$ is the transformation matrix

$$\mathbf{T}_3 = \begin{bmatrix} l_x & m_x & n_x \\ l_y & m_y & n_y \\ l_z & m_z & n_z \end{bmatrix}_{3\times 3}$$

where lk, mk and nk (k=x, y, z) are direction cosines

2D Plate properties

Type	Poisson's ration	Young's modulus	density	length	width	thickness
Steel	0.3	200e9	7700 kg/m3	0.3 m	0.3 m	0.006 m

Abaqus modeling

4 elements – 9 nodes

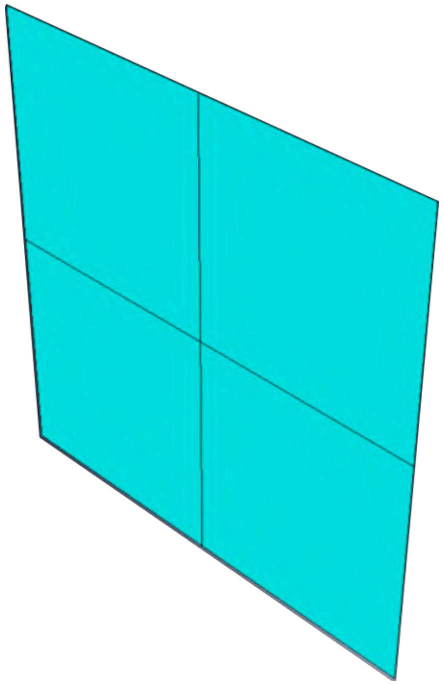

900 elements – 961 nodes

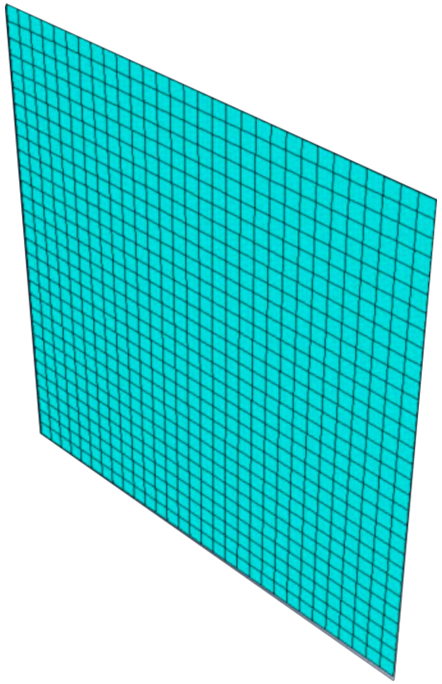

The plate was modeled in a free-free mode

Abaqus modeling (4 elements)

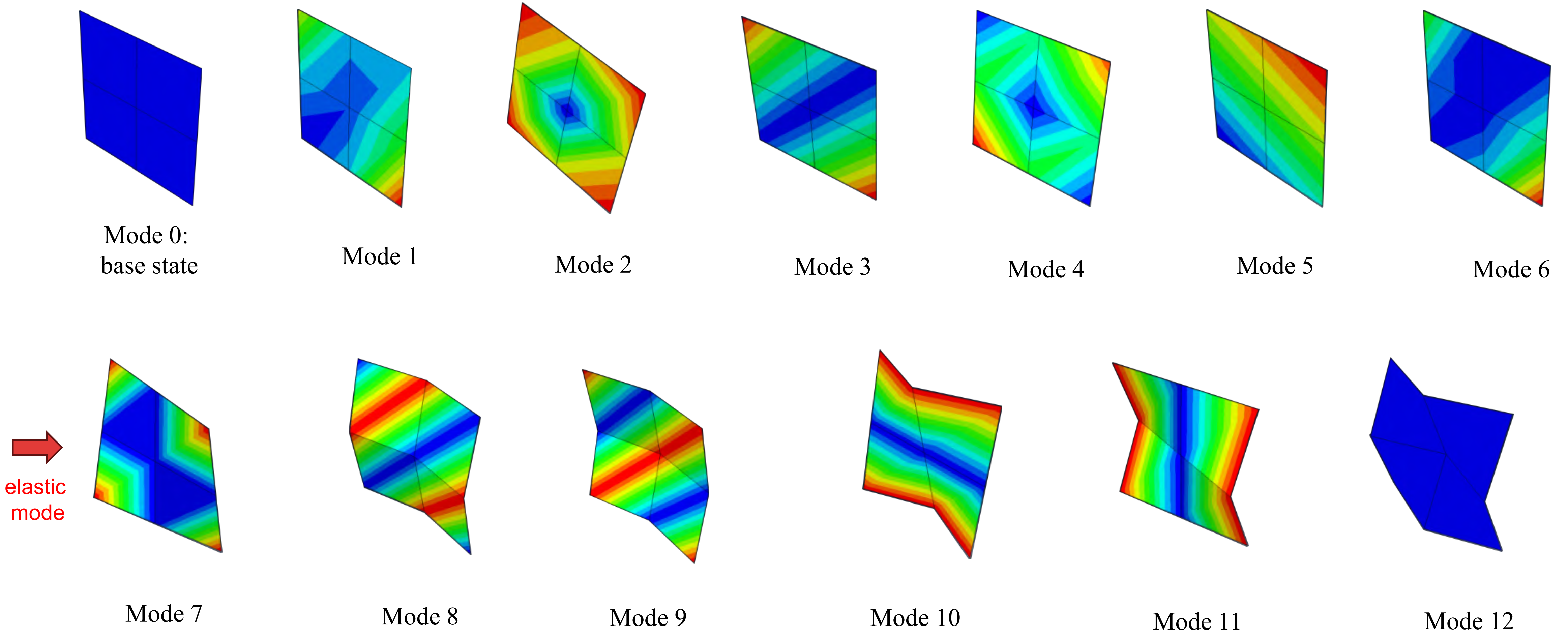

Abaqus modeling (900 elements)

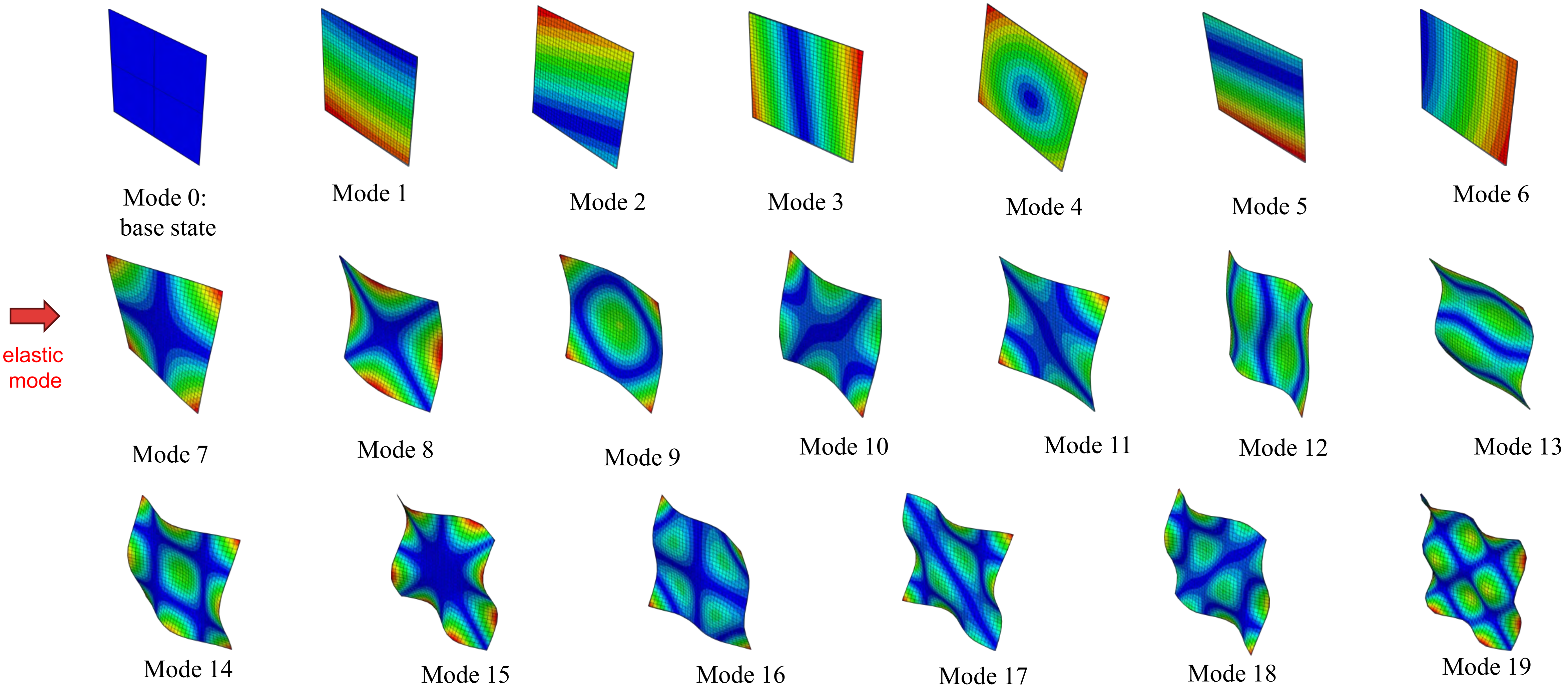

Mode Frequency

Step/Frame

Step Name	Description
Step-1	

4 elements

Frame

Index	Description			
0	Increment	0: Base State		
1	Mode	1: Value = -3.19909E-07 Freq =	0.0000	(cycles/time)
2	Mode	2: Value = -2.69152E-07 Freq =	0.0000	(cycles/time)
3	Mode	3: Value = -1.24332E-07 Freq =	0.0000	(cycles/time)
4	Mode	4: Value = -8.33534E-08 Freq =	0.0000	(cycles/time)
5	Mode	5: Value = -4.33065E-08 Freq =	0.0000	(cycles/time)
6	Mode	6: Value = -3.72529E-09 Freq =	0.0000	(cycles/time)
7	Mode	7: Value = 2.12713E+06 Freq =	232.12	(cycles/time)
8	Mode	8: Value = 5.66377E+06 Freq =	378.77	(cycles/time)
9	Mode	9: Value = 1.05068E+07 Freq =	515.89	(cycles/time)
10	Mode	10: Value = 1.41477E+07 Freq =	598.64	(cycles/time)
11	Mode	11: Value = 1.41477E+07 Freq =	598.64	(cycles/time)
12	Mode	12: Value = 3.52346E+07 Freq =	944.72	(cycles/time)

Step/Frame

Step Name	Description
Step-1	

900 elements

Frame

Index	Description			
0	Increment	0: Base State		
1	Mode	1: Value = 2.11708E-06 Freq =	2.31573E-04	(cycles/time)
2	Mode	2: Value = 3.40977E-06 Freq =	2.93888E-04	(cycles/time)
3	Mode	3: Value = 5.05996E-06 Freq =	3.58009E-04	(cycles/time)
4	Mode	4: Value = 6.18608E-06 Freq =	3.95847E-04	(cycles/time)
5	Mode	5: Value = 7.60294E-06 Freq =	4.38845E-04	(cycles/time)
6	Mode	6: Value = 1.44800E-05 Freq =	6.05625E-04	(cycles/time)
7	Mode	7: Value = 1.89263E+06 Freq =	218.95	(cycles/time)
8	Mode	8: Value = 4.05830E+06 Freq =	320.62	(cycles/time)
9	Mode	9: Value = 6.23002E+06 Freq =	397.25	(cycles/time)
10	Mode	10: Value = 1.26330E+07 Freq =	565.68	(cycles/time)
11	Mode	11: Value = 1.26330E+07 Freq =	565.68	(cycles/time)
12	Mode	12: Value = 3.95886E+07 Freq =	1001.4	(cycles/time)
13	Mode	13: Value = 3.95886E+07 Freq =	1001.4	(cycles/time)
14	Mode	14: Value = 4.20637E+07 Freq =	1032.2	(cycles/time)
15	Mode	15: Value = 5.01417E+07 Freq =	1127.0	(cycles/time)
16	Mode	16: Value = 6.26389E+07 Freq =	1259.6	(cycles/time)
17	Mode	17: Value = 1.15204E+08 Freq =	1708.3	(cycles/time)
18	Mode	18: Value = 1.15204E+08 Freq =	1708.3	(cycles/time)
19	Mode	19: Value = 1.46137E+08 Freq =	1924.0	(cycles/time)

Base state estimation with GE

Mode	Abaqus (4 element, 9_nodes)	Generalized Eigenvalue	Error (abs)
7	232.12	232.027	0.0093
8	378.77	379.044	0.274
9	515.89	515.983	0.0093
10	598.64	598.768	0.128
11	598.64	598.768	0.128
12	944.72	945.03	0.31

Single state change with GE and LEMP

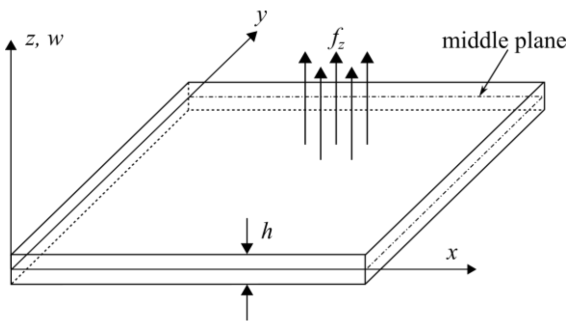

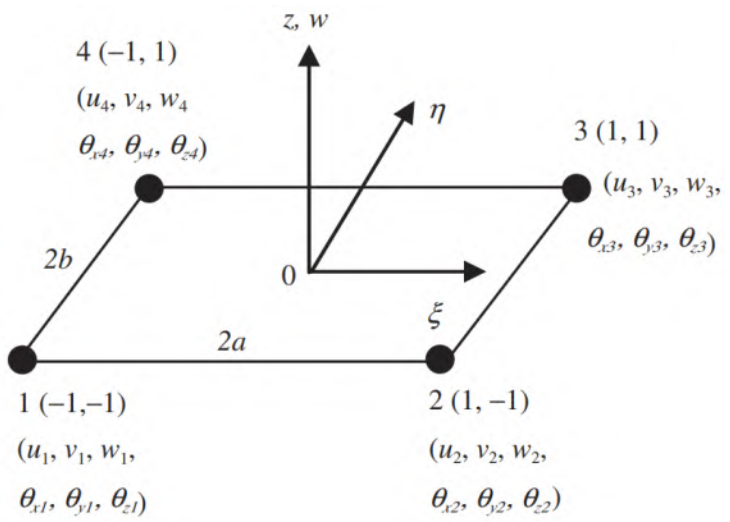

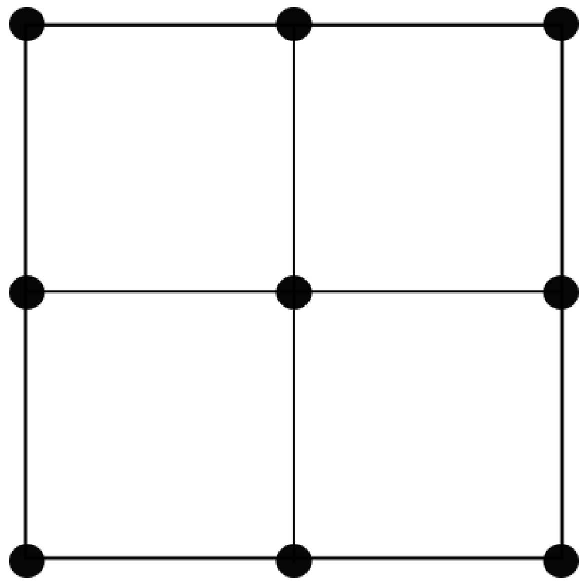

Single state change with GE and LEMP

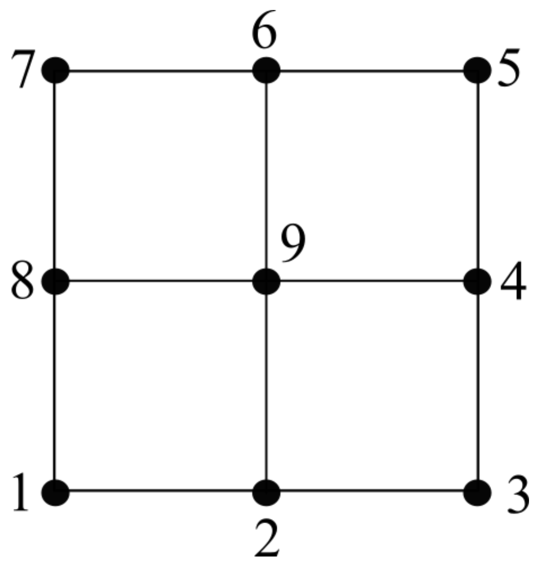

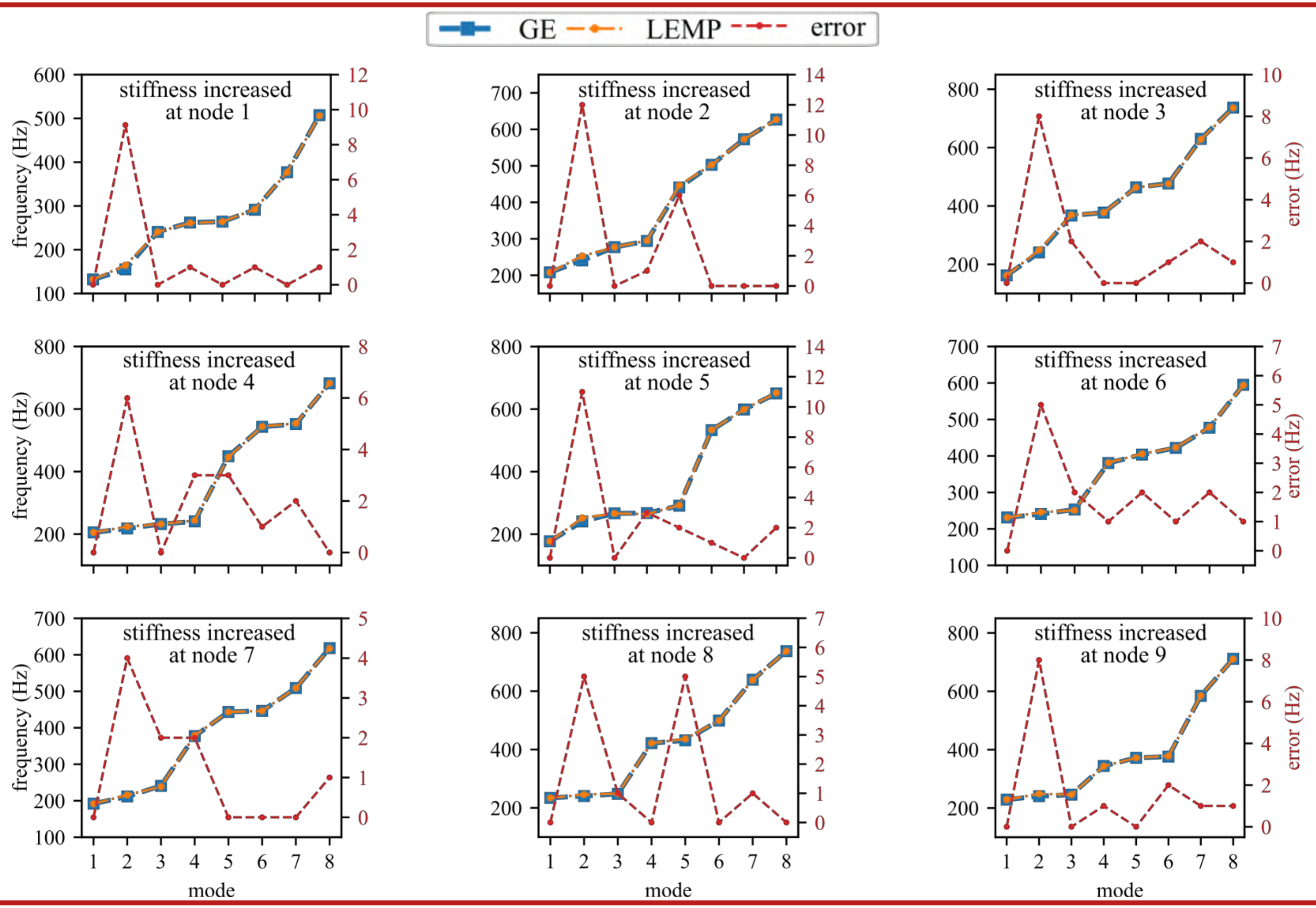

Increasing Stiffness value by 5e100 N/m at deflection (w) DOF of z-axis

Single state change with GE and LEMP

Model update accuracy and timing

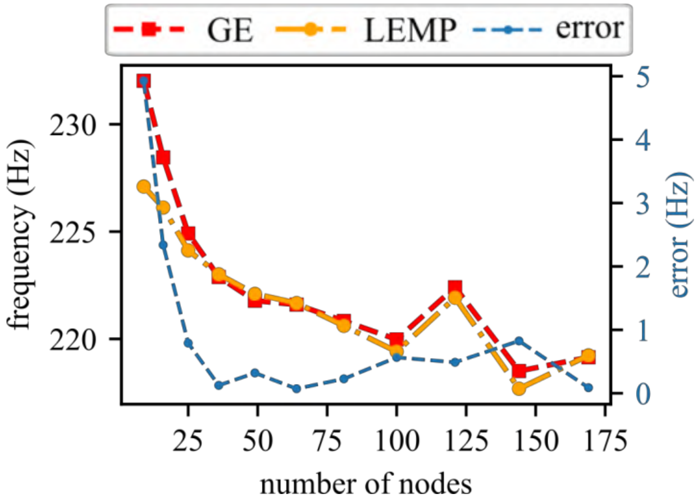

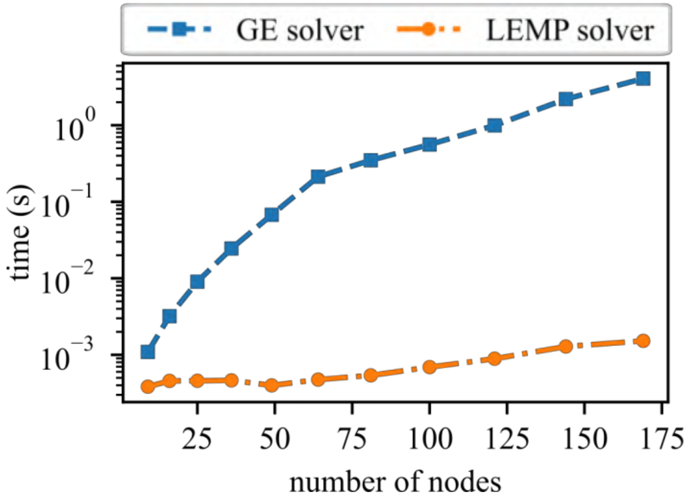

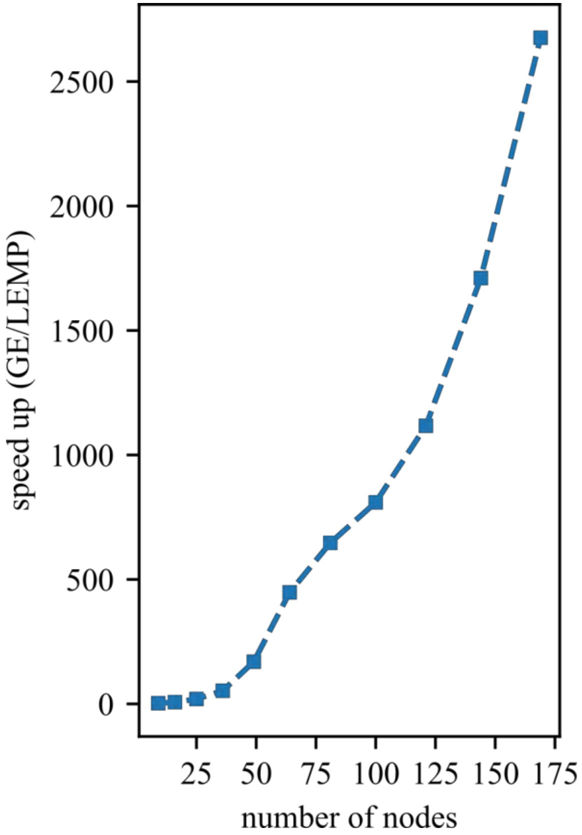

Only the first elastic mode was used for the frequency plot

Single state change with GE and LEMP

Estimation Timing for GE and LEMP

single change calculated using:				generalized eigenvalue		LEMP		
no. of nodes	no. of element	DOF	matrix size	freq (Hz)	time GE (s)	freq (Hz)	time LEMP (s)	error (Hz)
9	4	54	54 x 54	232.027	0.001093	227.099	0.000384	4.928
16	9	96	96 x 96	228.458	0.00320	226.120	0.000456	2.338
25	16	150	150 x 150	224.914	0.009031	224.123	0.000458	0.791
36	25	216	216 x 216	222.886	0.024529	223.01	0.000464	-0.124
49	36	294	294 x 294	221.78	0.067579	222.1	0.000399	-0.32
64	49	384	384 x 384	221.599	0.212773	221.67	0.000475	-0.071
81	64	486	486 x 486	220.837	0.348656	220.610	0.000539	0.227
100	81	600	600 x 600	219.975	0.559744	219.41	0.000691	0.565
121	100	726	726 x 726	222.409	0.994675	221.919	0.000890	0.488
144	121	864	864 x 864	218.505	2.197694	217.68	0.001285	0.825
169	144	1014	1014 x 1014	219.147	4.075451	219.234	0.001523	-0.087

Up to 100 nodes, the LEMP algorithm can still achieve 691 μs while GE is already at 0.56 s.

Conclusion

- The LEMP algorithm can be useful for faster solving of system equation for 2D structures because of large matrix size.

- LEMP accuracy compared to the Generalized Eigenvalue procedure is good.

- Alternative 2D model construction should be used before employing LEMP algorithm to solve the system equation.

Takeaway

- It is *possible* to use FEA models for micro-second tracking of structures during impact.

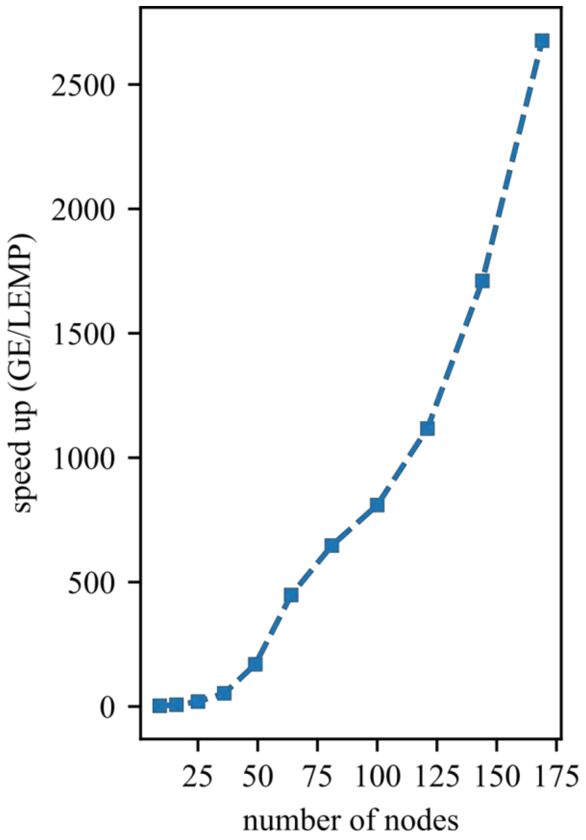

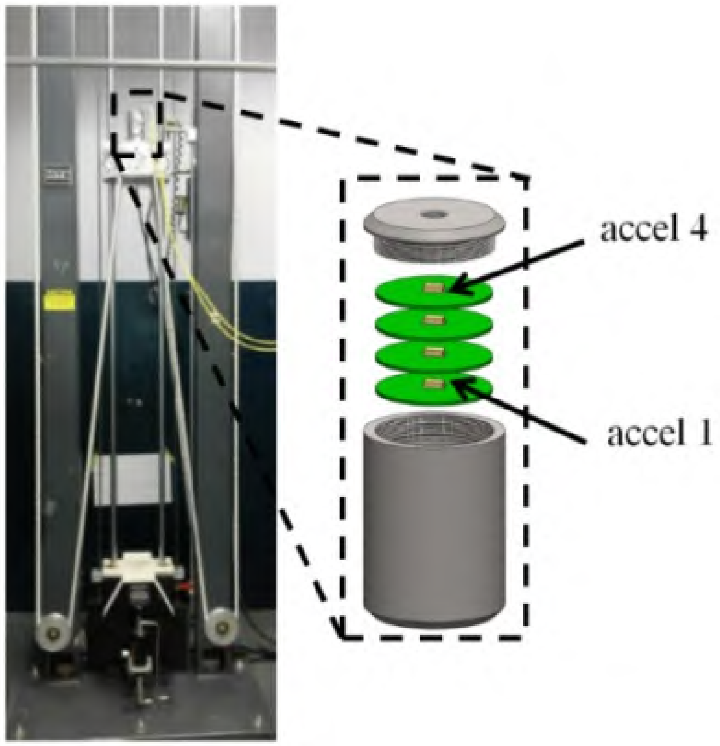

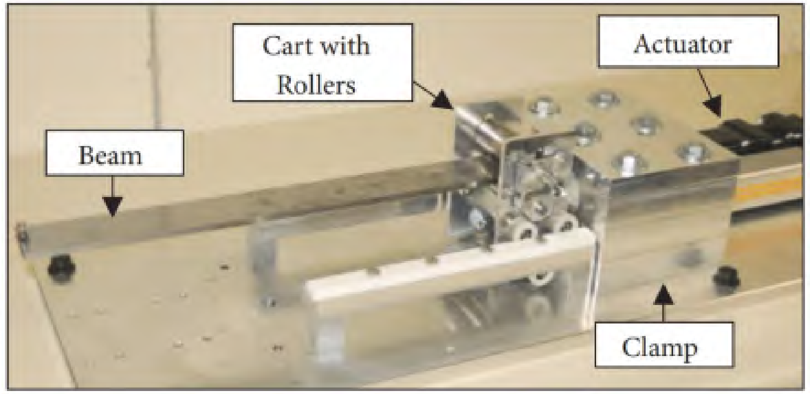

Acknowledgement

This material is based upon work supported by the Air Force Office of Scientific Research (AFOSR) through award no. FA9550-21-1-0083. This work is also partly supported by the National Science Foundation Grant numbers 1850012 and 1956071. The support of these agencies is gratefully acknowledged. Any opinions, findings, conclusions, or recommendations expressed in this material are those of the authors, and they do not necessarily reflect the views of the National Science Foundation or the United States Air Force.

THANKS!

Name: Emmanuel Ogunniyi
Title: Graduate Research Assistant
Email: ogunniyi@email.sc.edu
Social

South Carolina